Journal of Electroceramics, 12, 101–108, 2004

Micromachined Ultrasonic Transducers and Acoustic Sensors Based on Piezoelectric Thin Films

P. MURALT & J. BABOROWSKI
Ceramics Laboratory, Swiss Federal Institute of Technology EPFL, CH-1015 Lausanne, Switzerland

Abstract. A review is given on the current state of the art in piezoelectric micromachined ultrasonic transducers (pMUT). It is attempted to quantify the limits of pMUT's with respect to the electromechanical coupling, and to relate current achievements. Main needs for future research are identified in design, micromachining and further improvements of PZT films. Applications are shortly reviewed.

Keywords: piezoelectric thin films, microsystems, acoustic sensors

1. Introduction

Ultrasonic transducers are best known for their applications in medical ultrasonic imaging (see, e.g., [1]). For this purpose, an ultrasound wave is emitted into the body by a transmitter. The intensities of waves reflected from the various parts of the body are measured as a function of time by a receiver. Transmitter and receiver function can be delivered by the same device if the excitation and reception are separated in different time windows. The applied frequency depends on the depth of the investigated organs, and amounts to 3 to 5 MHz for deep organs, 15 MHz for eyes, and up to 50 MHz for skin, artery walls, and other thin tissues. The excitation signal is either a pulse (pulse-echo method) or a continuous wave. In the first case, the pulse contains a broad frequency range, and the imaging is based on the intensities and delay times with which reflected wave packets are captured by the receiver. In the second case the frequency band is narrow. Frequency shifts due to the Doppler effect at moving parts can be observed. In order to get efficient excitation and sensitivity, the devices are operated at resonance. However, short pulses, or equivalently broad emission bands, are only achieved if the quality factor Q is small (The acoustical Q of an echographic transducer should be less than one [2]). The receiver should of course be very sensitive and thus efficiently transform the received mechanical power into an electrical signal. For this purpose a large coupling coefficient (k^2) is required. Doppler shift measurements require narrower bands, and thus allow for larger Q factors. However, in the practice, the same probe should cover both operating methods. At present, ultrasound transducers are based on piezoelectric $\lambda/2$ bulk wave resonators. The piezoelectric material is an optimized PZT ceramics. Modern transducers are linear arrays in order to perform beam steering and shaping, and to increase resolution. The optimal element density is two per sound wavelength of the investigated medium. In medical applications this corresponds to a pitch of about 300 μm for deep organs, 100 μm for eyes, and 30 μm for thin tissue investigations.

There are several other applications of ultrasound in sensors and materials testing. Closely related to medical imaging are acoustic microscopy and nondestructive testing. The main differences are related to the fact that the acoustic impedances, sound velocities, and acoustic damping of the investigated materials are different from the ones of the human body, requiring adaptions of geometries and frequencies. The pulse-echo method is also applied in sensors to measure distances or to detect the presence of an object, similar to the ultrasonic "vision" system of bats. Doppler shift measurements are used in flow meters measuring liquid flows. Gas detectors can be made using the principle of resonating cavities, whose resonance frequency depends on the sound velocity of the gas in the cavity [3]. Microphones fall also into the category of sensors

for acoustic waves. Finally, there are actuators based on ultrasonic excitation, such as ultrasonic motors and droplet ejectors as used in ink jets. Both have been realized as micromachined versions [4, 5].

In the recent years, micromachined versions of transducers attracted very much interest [6–10]. In some cases it is motivated by integrating a MUT directly onto a CMOS chip [11]. The main reason for imaging is the prospect to dispose of 2-dimensional arrays offering excellent beam steering (phased array operation), high-resolution and real-time imaging capabilities. It is clear that micromachining techniques allow for a much higher precision than the reticulation techniques used for the fabrication of bulk ceramics elements. This is especially true for transducers operating above 10 MHz. Although progress has been made in reticulation techniques [12], the wiring of 2-d transducers is difficult to solve in case of reticulated ceramics. Silicon micromachining is quite advanced in the fabrication of deep through holes [13, 14] and buried conductor lines needed to realize wiring of 2-d arrays. So it seems to be quite clear that the interconnect part of a 2-d array will be fabricated by means of silicon micro machining (realized in a "connectic" waver). The question is whether the acoustic part is made as well in silicon technology—in this case the joining of the two parts is a mastered problem—or whether the acoustic part looks more like a reticulated ceramics (hybrid approach). The latter approach has indeed been successfully realized in case of pyroelectric focal plane arrays for infrared vision systems [15] based on a ceramic (Ba,Sr)TiO_3 ceramics.

For the pure silicon micromachining approach, electrostatic as well as piezoelectric thin film structures are investigated (see Fig. 1). Both are based on membrane structures. A priori, these have an advantage for medical applications: Membranes are much softer than bulk PZT and match better the acoustic impedance of soft matter. Most important advantage of capacitor type structures (capacitive micromachined ultrasonic transducer cMUT) is the high coupling coefficient. Close to the collapse, 100% conversion efficiency is theoretically calculated (see, e.g. [16]). Although impossible to operate too close to the collapse, the practically achievable values are quite large. Coupling coefficients of more than 70% have been demonstrated [17, 18]. One of the reasons for the large coupling is the fact that the electrostatic force acts vertical to the membrane, i.e. parallel to the membrane deflection and force output. In piezoelectric materials or structures, the coupling coefficient k^2 is defined as the ratio of stored mechanical energy to the stored electrical energy. k^2 depends on the stiffness of the material or the spring constant of the structure. This is also the case for piezoelectric MUT's (see below). In cMUT's, however, the effective spring constant softens with increasing voltage and becomes zero at the collapse voltage [19]. The coupling coefficient in this case must be rather understood as the ratio of the available mechanical work to the electrical energy delivered to the device. In piezoelectric devices the available work depends very much on the matching. In pMUT's, the exploited effect is based on the transverse coupling k_p. The piezoelectric force is in fact in the membrane plane, thus perpendicular to the force to be delivered. The mechanism to turn the output force by 90° is the bending of the membrane by the transverse piezoelectric stress or strain (see Fig. 1). Bimorph structure and hetero-morph structures can be applied. The latter contains a passive layer (Si, Si_3N_4, etc.). In order that this mechanism works well, the neutral plane of the membrane must not lie within the piezoelectric film. Otherwise the lower part of the film would work against the upper part of the film. It should be in the passive material. Using hand waving arguments, we

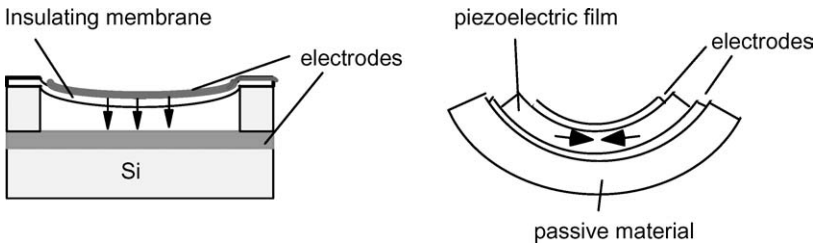

Fig. 1. Schematic cross section through (a) electrostatic and (b) piezoelectric MUT structure. The arrows indicate the direction of the force developed by the driving principle.

can say that in the best case the coupling coefficient of a piezoelectric heteromorphous membrane amounts to $k^2 = k_p^2/2$ since half of the vibrating structure is passive. In bulk PZT, k_p amounts to 60% typically, which is 10 to 20% less than k_{33} used in bulk transducers. The best possible coupling coefficient amounts thus to about $k = 42\%$ ($k^2 = 18\%$). So even if one argues that the better acoustic matching would correspond to a $k^2 = 36\%$ for a bulk transducer, we still miss by a factor 1.5 the effective coupling of today's probes. This figure possibly might be acceptable for high resolution, high frequency probes. The question remains, whether the above optimistic numbers are reached or not, and whether there are other applications that do not need such a high coupling. This paper will give a short review on pMUTs and tries to answer some of the questions.

2. Clamped Plate Structure

The above optimistic estimation is based on a piezoelectric laminated plate that is freely suspended. This means that there is no force acting on the border of this plate. An estimation of the coupling factor for this case is given in Ref. [20]:

$$k^2 \approx 6\frac{1-\nu}{Y}\frac{e_{31,f}^2}{\varepsilon_0\varepsilon_{33,f}}\frac{t_p}{h}, \quad t_p < h/2 \tag{1}$$

where the thickness of the piezoelectric material t_p must be smaller than half the total thickness h. Y and ν are Youngs modulus and Poisson ratio of the passive material, $e_{31,f}$ is the effective transverse piezoelectric coefficient $e_{31,f} = d_{31}/(s_{11}^E + s_{12}^E)$ that is easily determined from thin film structures [21, 22]. Taking silicon as passive material, considering an $e_{31,f}$ of 12 C/m^2 that applies for dense PZT{100} films [23], we arrive at $k^2 = 16\%$ for $t_p = 0.4$ h This value is in fact close to the first estimation.

The essential point of micro machining and design is to solve this problem of turning the output force by 90°. The simplest possibility, which is also best understood in the frame of analytical mathematics, is the clamped disk or plate (The first derivative of the deflection function is zero at the border of the plate). A flexural resonance is excited as schematically shown in Fig. 2. The whole structure consists of a few films with a minimal amount of patterning steps. The membrane is either liberated by surface micromachining (as shown in Fig. 2) or by bulk micromachining. The first such structures containing PZT films have been fabricated for micromachined ultrasonic stators for micromotors [4, 24]. They also have been applied for the first demonstrations of ultrasonic imaging with pMUTs [9]. Such plate structures can be handled by analytical mathematics if it is assumed that the deflection is small as compared to the diameter of the plate. The problem is usually solved for radial symmetrical structures. Solutions have been calculated following Kirchhoff's plate theory by implementing the equation of state of the piezoelectric material into a multilayered plate obeying the plate equation, the boundary conditions for clamping, and the electrode geometries. Differential equations or complete plate equations have been derived [25, 26], or in a more approximate way using the energy method [27, 28], which in fact goes also back to Kirchhoff [29]. In this case, the elastic energy is numerically calculated based on the deflection functions of the fundamental resonance (Bessel functions). Stiffness and position of the neutral plane are calculated according known algorithms [30]. Using the latter method, k^2 has been calculated for various thickness values of PZT as a function of the thickness of the passive part as shown in Fig. 3.

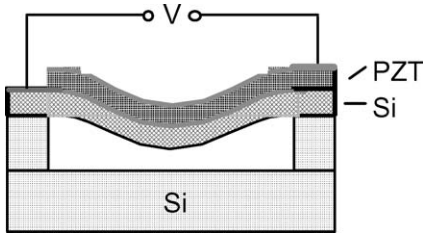

Fig. 2. Schematic cross section through clamped plate.

The maximal coupling is achieved when the Si layer is slightly thicker than the PZT film. The curves show that the coupling is drastically reduced when the neutral plane is situated inside the PZT material. The maximal value does not increase much with PZT film thickness, and saturates at about $k^2 = 3.5\%$. However, the maximum becomes broader with increasing thickness. In addition, the peak values are less reduced by film stresses that may stretch the membrane and may reduce very much the peak in coupling coefficient. Stretching forces add a correction term to k^2 proportionally to a^2/h^3 (a: plate radius, [27]). With increasing thickness h, the influence of stretching is thus dramatically reduced. The resonance frequency increases roughly as

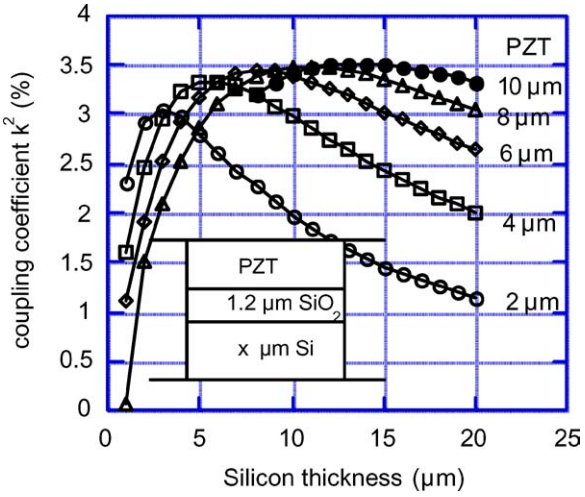

Fig. 3. Simulation results of k^2 for the basic deflection mode in case of a stress free diaphragm of 300 μm diameter with a centered electrode having the optimal diameter of 65% of the plate diameter. PZT film parameters: $e_{31,f} = 12$ C/m^2, $\varepsilon_{33,f} = 1200$. The calculations are explained in Ref. [28].

$f_0 \propto h/a^2$. If the application defines the size of the plate (as e.g. the pitch of an array) and the frequency, the thickness of PZT and silicon are fixed by the condition of maximal coupling. The PZT film thickness has—of course—a direct impact on the amplitude and the output force in the emitter mode, and on signal voltage and signal-to-noise in the receiver mode.

Above calculations show that the clamped plate is not an ideal realization of a flexural transducer. The clamping of the plate reduces the coupling factor considerably. Comparing Eq. (1) with Fig. 3 we note that there is a difference of a factor 4 in k^2. Other types of micromachined structures must be found to approximate the free plate.

3. Approximating Freely Suspended Plates

The free plate is best approximated by a structure keeping the plate in the center. The whole border would be free to move. However, it is not evident how to mount the electrical connections to such a structure. It is much easier to keep the membrane by a number of bridges around the border and leave the center free to move. The realization of such a bridge is shown in Fig. 4. (see Ref. [31] for fabrication details).

An improved control of the membrane thickness is achieved by means of SOI wafers. Such a wafer contains a silicon layer of defined thickness separated from the bulk wafer by a buried oxide layer. The latter serves as etch stop layer and allows the fabrication of very homogeneous silicon membranes of well-defined thickness. Figure 5 shows the admittance curve of a 300 μm plate laminated with a 2 μm thick PZT film, obtained from a SOI substrate [33]. The coupling coefficient was derived from an equivalent circuit model (as depicted in Fig. 5): $k^2 = CN^2/C_0$. The parasitic capacities due to wiring should be minimized, otherwise these parasitics add to C_0. k^2 was obtained as 5.3%, which is considerably larger than the expected result of a clamped plate (2.9% according to Fig. 3). For the interpretation we have to include the fact that a bias voltage was applied. This increases $e_{31,f}$ and decreases the dielectric constant. (At equivalent films, an increase of $d_{33,f}$ by 35% has been measured at 100 kV/cm [23]). The coupling increases accordingly. Figure 6 shows the increase of k^2 as a function of bias field (different device). The calculated 2.9% could well increase by 80% to 5.2% considering the bias of 100 kV/cm as applied for the measurement of Fig. 5. The increase by partial liberation of the plate appears to be rather marginal. More designs and measurements are needed to clarify this point.

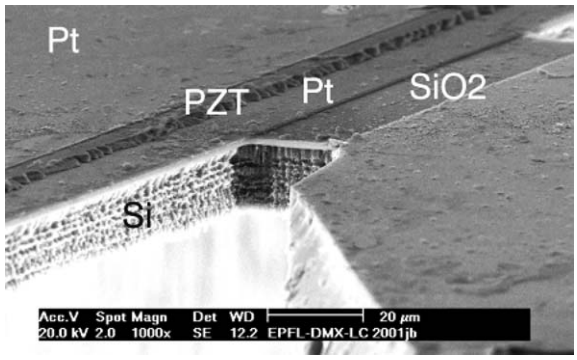

Fig. 4. SEM viewgraph showing the micromachined bridge of a suspended membrane with the etched Pt/PZT/Pt sandwich. The membrane was obtained by thinning the silicon down from the backside by deep silicon etching. The final thickness was defined by time control (from Ref. [32]).

4. Emission Power

The emission power of an ultrasonic device is an additional important parameter. In case of good acoustic matching the emitted power should approach the

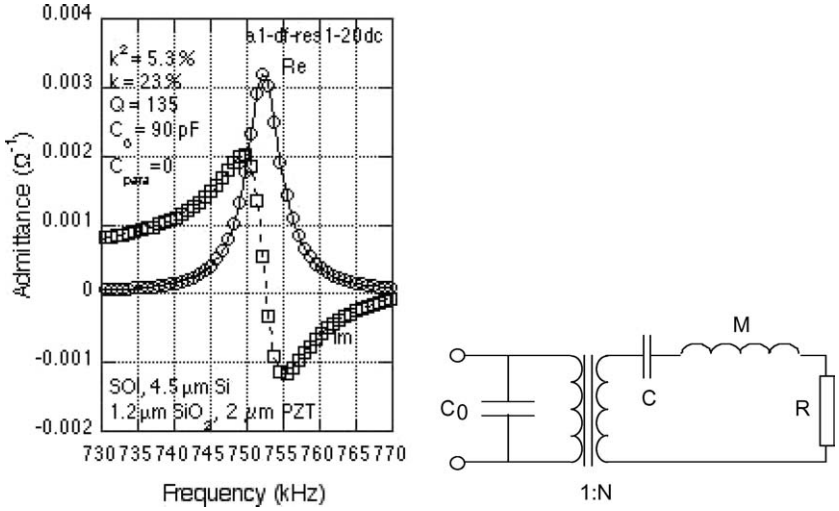

Fig. 5. Admittance curves of 300 μm diameter, round, suspended, single transducer at 100 kV/cm dc bias field (from Ref. [33]), together with the equivalent circuit model used for the derivation of parameters.

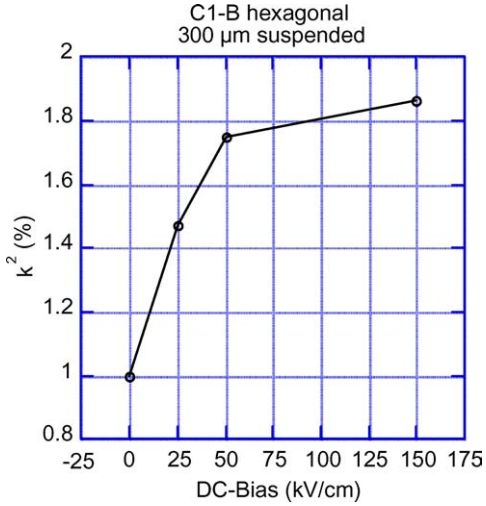

Fig. 6. Increase of small signal coupling by the application of a bias voltage (from Ref. [34]).

mechanical power P_{mech} in the vibrating structure:

$$P_{\text{mech}} = k^2 P_{\text{el}} = k^2 \omega C_0 U_{\text{rms}}^2 \qquad (2)$$

where ω is angular frequency and U_{rms} the root mean square voltage applied to the capacitor. Thin films usually dispose of quite large break-down fields. So in principle one can operate the device at much larger fields E_{rms} than what is applied in case of bulk transducers (about 10 times larger). The energy density $\varepsilon_0 \varepsilon_r E_{\text{rms}}^2$ may be increased substantially and compensates to a certain extent the smaller thickness of the piezoelectric materials and lower coupling coefficient. In this way, relatively large output powers are achievable and the power specifications are met in theory [34]. However, there is a price to pay: an increased loss due to dielectric loss (small signal) or hysteretic behavior (large signal). This issue requires special attention in order to avoid overheating of the device.

5. Quality Factor—Immersed Operation

The pMUT's seem to give inherently high quality factors when operated in air. The example shown in Fig. 5 (wavelength in air/diameter = 1.3) yielded a Q-factor of 135, the $k^{2*}Q$ product amounted to 7.2. When immersed into a liquid the Q-factor decreases considerably. Figure 7 shows the admittance of a 1 mm diameter transducer in air and in Fluorinert (an electrically insulating liquid) [33]. The Q-factor decreased by a factor 5. Given that the sound velocity in fluorinert is 600 m/s, the 19 kHz resonance corresponds to a wavelength of 32 mm, i.e. a value much larger than the device diameter of 1mm. In this regime, the impedance of the liquid is low and mostly reactive [35], explaining the large Q observed. Figure 8 shows a 450 μm element of a 16 element array. In this case the resonance in

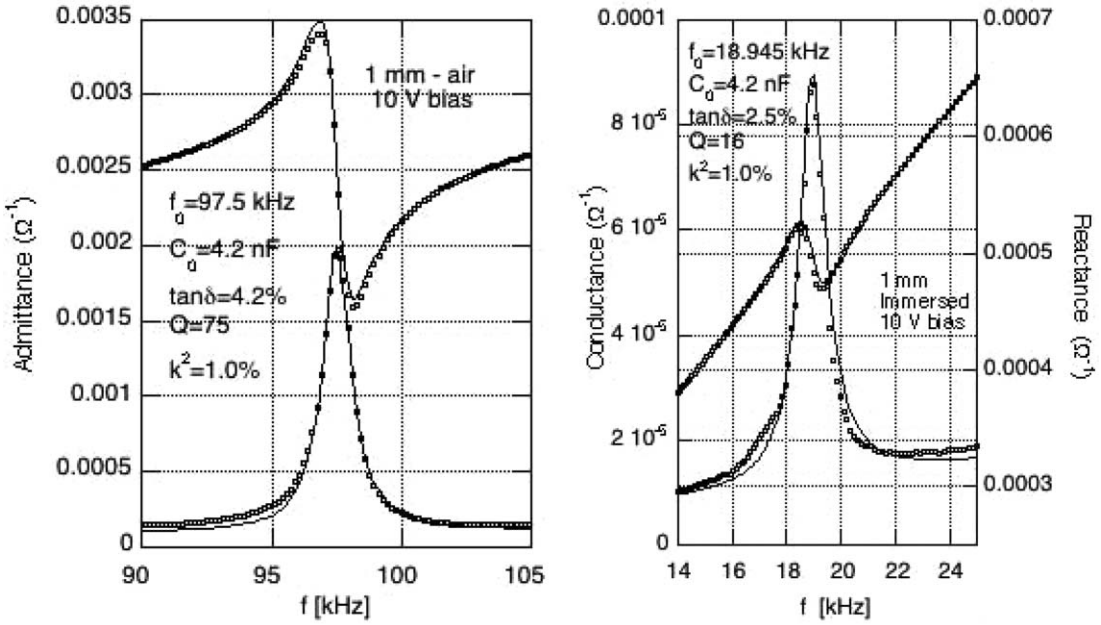

Fig. 7. Admittance curves of 1000 μm diameter, round, suspended, single transducer at 50 kV/cm dc bias field: (a) in air; (b) in Fluorinert. The full line is a fit to the equivalent circuit model (from Ref. [33]).

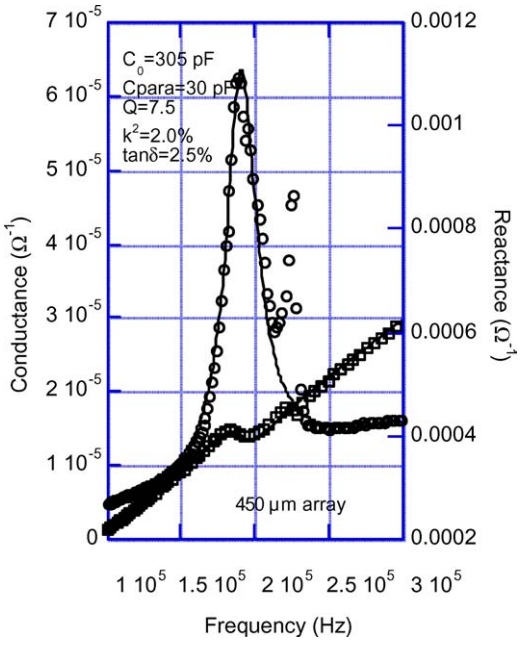

Fig. 8. Admittance curves of round, suspended pMUT immersed in Fluorinert. (Diameter: 450 μm, silicon thickness: 5 μm, PZT thickness: 2 μm). It is part of a linear array of 16 elements.

fluorinert is at 190 kHz, corresponding to a wavelength of 3.2 mm. The reduction in Q anounts to a factor 6. Most interesting is the modal behavior in immersion. Simulation calculations show that it might be possible to enlarge the bandwidth due to higher modes that are getting close to the basic mode in the liquid [32].

6. Discussion and Outlook

The processes available today allow for the fabrication of planar pMUT structures with few micrometer thick PZT films. While such pMUT's may achieve theoretically coupling factors of about $k^2 = 20\%$, as argued earlier in this paper, the best coupling factors achieved to date amounts to 6%. Improvements of the material seem to be still possible. Comparing the $e_{31,f}$ of PZT films with best ceramics data [23], and prospects with other solid solution systems of $PbTiO_3$ (see [36]), an improvement of this coefficient by 50% looks realistic. This means a factor two increase of k^2. Bimorph structures have to be considered as well. They could be suitable to increase the sensitivity, or the bandwidth in reception, due to the fact that bimorphs exhibit a larger piezoelectric part in the vibrating structure. For

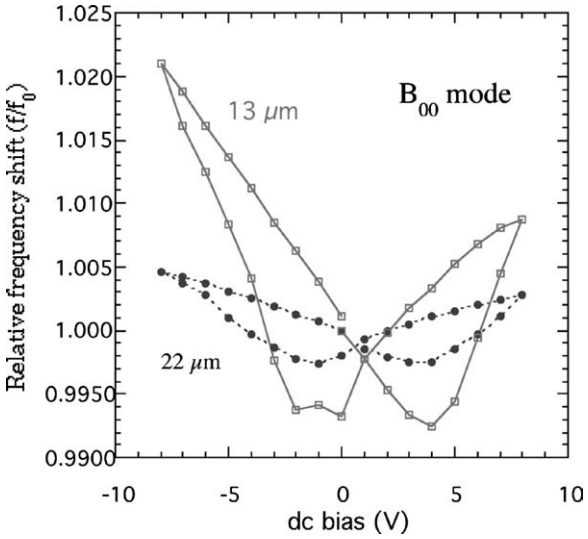

Fig. 9. Frequency shift of the fundamental resonance by piezoelectric stresses. Plate diameter: 2 mm; PZT thickness: 0.5 μm; silicon thickness: 13 and 22 μm, electrode: concentric with diameter of 1 mm (from Ref. [27]).

the emission they do not improve much, since one cannot apply much field opposite to the polarization without switching. So the compressive piezoelectric stresses are limited in value. This can be seen from the frequency shift induced by the piezoelectric stress ($e_{31,f}$) as shown in Fig. 9. The up-shift corresponds to tensile stress when the electric field is parallel to the polarization, the down-shift to compressive stress when the electric field is anti-parallel to the polarization. The frequency shift is proportional to the piezoelectric stress [27]. Further improvements can be expected with optimized designs to approach an ideal suspended structure. There is, however, a further issue to solve. In the present design, we opened the membranes to increase the vibration amplitudes. For immersed operation, it is necessary to seal them again. Ideally, sealing should be done by polymer film. A further idea to increase bandwidth in liquids consists in overlapping resonance modes [37]. Important are simulation calculations to predict the modal behavior in liquids [38] and with sealing layers.

There is finally the question about applications that do not require large bandwidths. Applications of the current performance of pMUT's are conceivable for proximity and presence sensors working on short distances [39]. Transmit-receive experiments between micromachined pMUT's showed large responses up to several centimeters in air, and a few centimeters in Fluorinert [33]. Further applications include droplet ejectors [40], and acoustic sensors for chemical analysis [41].

Acknowledgments

This work was supported by the European Program "Growth/Innovative Products" and the Swiss Office for Education and Research OFES in the frame of the project "PARMENIDE". The authors would like to thank all the partners of this project, particularly to N. Ledermann from our laboratory, J.-F. Gelly from Thales-Microsonics, and D. Schmitt from the Frauenhofergesellschaft IBMT.

References

1. J.C. Bamber and M. Tristam, *The Physics of Medical Imaging*, edited by S. Webb (Adam Hilger: Bristol, 1988), p. 319.
2. J.L. Vernet, W. Steichen, R. Lardat, O. Garcia, and J.F. Gelly, *IEEEE Ultrasonic Symposium* (IEEE, Atlanta USA, 2001).
3. V. Mecea, *Sensors and Actuators B*, **15/16**, 265 (1993).
4. P. Muralt, M. Kohli, T. Maeder, A. Kholkin, K.G. Brooks, N. Setter, et al., *Sensors and Actuators A*, **48**, 157 (1995).
5. G. Percin, T.S. Lundgren, and B.T. Khuri-Yakub, *Appl. Phys. Lett.*, **73**, 2375 (1998).
6. M.I. Haller and B.T. Khuri-Jakub. *IEEE Ultrasonic Symposium* (1994).
7. M.I. Haller and B.T. Khuri-Jakub, *IEEE Trans. UFFC*, **43**, 1 (1996).
8. H.T. Soh, I. Ladabaum, A. Atalar, C.F. Quate, and B.T. Khuri-Jakub, *Appl. Phys. Lett.*, **69**, 3674 (1996).
9. J.J. Bernstein, S.L. Finberg, K. Houston, L.C. Niles, H.D. Chen, L.E. Cross, et al., *IEEE Trans. UFFC*, **44**, 960 (1997).
10. O. Oralkan, X. Jin, L. Degertekin, and P. Khuri-Yakub, *IEEE Trans. UFFC*, **46** (1999).
11. P.C. Eccardt and K. Niederer, *Ultrasonics*, **38**, 774 (2000).
12. R. Farlow, W. Galbraith, M. Knowless, and G. Heyward, *IEEE Trans. UFFC*, **48**, 639 (2001).
13. S.J. Ok, C.H. Kim, and D.F. Baldwin, *IEEE Trans. Adv. Packaging*, **26**, 302 (2003).
14. X.G. Li, T. Abe, X.Y. Liu, and M. Esashi, *J. Microelectromech. Systems*, **11**, 625 (2002).
15. C.M. Hanson, *Semiconductors and Semimetals*, **47**, 123 (1997).
16. A.S. Ergun, G.G. Yaralioglu, and B.T. Khuri-Yakub, *J. Aerospace Eng.*, **April 2003**, 76 (2003).
17. J. Johnson, O. Oralkan, U. Demirci, S. Ergun, M. Karaman, and P. Khuri-Yakub, *Ultrasonics*, **40**, 471 (2002).
18. G.G. Yaralioglu, A.S. Ergun, B. Bayram, E. Haeggstrom, and B.T. Khuri-Jakub, *IEEE Trans. UFFC*, **50**, 449 (2003).
19. F.V. Hunt, *Electroacoustics: The Analysis of Transduction and its Historical Background*, 2nd edition Harvard University Press: Cambridge MA, 1982.

20. P. Muralt, *Integrated Ferroelectrics*, **17**, 297 (1997).
21. M.-A. Dubois and P. Muralt, *Sensors and Actuators A*, **77**, 106 (1999).
22. J.F. Shepard, P.J. Moses, and S. Trolier-McKinstry, *Sensors and Actuators A*, **71**, 133 (1998).
23. N. Ledermann, P. Muralt, J. Baborowski, S. Gentil, K. Mukati, M. Cantoni, et al., *Sensors and Actuators A*, **105**, 162 (2003).
24. A.M. Flynn, L.S. Tavrow, S.F. Bart, R.A. Brooks, D.J. Ehrlich, K.R. Udajakumar, et al., Piezoelectric micromotors for microrobots, *J. Microelectromechanical Systems*, **1**, 44 (1992).
25. G. Percin and B.T. Khuri-Yakub, *IEEE Trans. UFFC*, **49**, 573 (2002).
26. G. Percin, *IEEE Trans. UFFC*, **50**, 81 (2003).
27. P. Muralt, A. Kholkin, M. Kohli, and T. Maeder, *Sensors and Actuators A*, **53**, 397 (1996).
28. M.-A. Dubois and P. Muralt, *IEEE Transactions on Ultrasonics, Ferroelectrics and Fequency Control*, **45**, 1169 (1998).
29. I. Szabo, *Höhere Technische Mechanilk*. Springer: Berlin, Göttingen, Heidelberg, 1956.
30. J. Söderquist, *J. Micromech. Microeng.*, **3**, 24 (1993).
31. J. Baborowski, *J. Electroceramics* (2003).
32. P. Muralt, D. Schmitt, N. Ledermann, J. Baborowski, P.K. Weber, W. Steichen, et al. *IEEE Ultrasonic Symposium* (Atlanta, USA, 2001).
33. J. Baborowski, N. Ledermann, and P. Muralt. *IEEE Ultrasonic Symposium* (Munich, Germany, 2002).
34. P. Muralt, D. Schmitt, N. Ledermann, J. Baborowski, P.K. Weber, W. Steichen, et al. *IEEE Ultrasonics conference 2001*, IEEE (Atlanta, USA, 2001).
35. D. Royer and E. Dieulesaint, *Ondes elastiques dans les solides*. Vol. 1, Masson, Paris 1996.
36. S. Troyler-McKinstrey and P. Muralt, see this issue, (2003).
37. J. Baborowski, N. Ledermann, P. Muralt, and D. Schmitt, *Int. J. Comp. Eng. Sci.*, **4**, 471 (2003).
38. J.F. Gelly, F. Lanteri, and S. Ballandras, *3rd MUT Workshop*, Lausanne (2003).
39. K. Yamshita, H. Katata, M. Okuyama, H. Miyoshi, G. Kato, S. Aoyagi, et al., *Sensors and Actuators A*, **97/98**, 302 (2002).
40. G. Percin and B.T. Khuri-Yakub, *Review of Scientific Instruments*, **73**, 2193 (2002).
41. N. Ledermann, J. Baborowski, A. Seifert, B. Willing, S. Hiboux, P. Muralt, et al., *Integrated Ferroelectrics*, **35**, 177 (2001).